Environmental Science Processes & Impacts

ROYAL SOCIETY OF CHEMISTRY

PAPER

View Article Online
View Journal | View Issue

Cite this: *Environ. Sci.: Processes Impacts*, 2025, **27**, 2698

Environmental stability characteristics of the immobilization effect of sulfhydryl grafted palygorskite on soil-available cadmium†

Miao Wang, Xusheng Gao, Xilin Chen, Yifei Shu, Qingqing Huang, Lin Wang, Xu Qin, Yuebing Sun, Yujie Zhao and Xuefeng Liang *

The stability of heavy metal immobilization amendments represents a critical factor in evaluating remediation effectiveness. To comprehensively investigate the environmental stability of a novel amendment, sulfhydryl grafted palygorskite (SGP), a series of experiments encompassing chemical exposure and sorption, incubation with simulated acid rain and thermal variations, and field validation were conducted. SGP demonstrated chemical stability across diverse media, including ambient atmosphere, aqueous solutions (H_2O, $CuSO_4$, and H_2O_2), and heterogeneous soil matrices, as evidenced by a maximum relative standard deviation of changes in the free sulfhydryl content and a sorption capacity below 5%. Simulated acid rain leaching resulted in a maximum cumulative leaching efficiency of less than 1%, revealing no significant impact on Cd^{2+} release from SGP-amended soil and confirming its resistance to acid rain. Thermal variance tests (−20 °C to 60 °C) demonstrated temperature-insensitive performance characteristics, with fluctuations below 10% observed in soil-available Cd regulation and Cd uptake by pakchoi. Field demonstrations in acidic and alkaline soils validated the universal stability of SGP over two years, with soil-available Cd reductions of 47.2–76.4% and grain Cd content reductions of 38.1–78.3% across seasonal variations. This study qualitatively and quantitatively assessed the stability characteristics of the SGP immobilization effect, providing theoretical support for developing new immobilization amendments and the safe utilization of contaminated farmland.

Received 5th April 2025
Accepted 13th July 2025

DOI: 10.1039/d5em00262a

rsc.li/espi

Environmental significance

Soil contamination with Cd has become a major environmental issue for food security and sustainable agriculture in China. Chemical immobilization is widely adopted for the safe utilization of heavy metal contaminated farmlands, but it only alters metal speciation rather than removing heavy metals from the soil. There is a risk of remobilization and release due to aging processes influenced by various environmental factors. The environmental stability poses a challenge for the practical implementation of immobilization. Sulfhydryl grafted palygorskite (SGP), as an emerging amendment, has been designated as a first-level amendment by the Joint Research Group on Heavy Metal Pollution Remediation of the Ministry of Agriculture and Rural Affairs of China. Numerous studies have validated its efficacy in immobilizing bioavailable Cd in alkaline soil. Despite these advancements, the environmental stability and interference resistance of the sulfhydryl-modified amendment remain inadequately understood.

1 Introduction

Heavy metal contamination in Chinese soils has garnered significant attention owing to its environmental and ecological risks as well as its potential threats to agricultural product quality and human health.[1] Currently, chemical immobilization is widely adopted for the safe utilization of heavy metal contaminated farmlands in China.[2] In major rice-producing regions of southern China, diverse immobilization amendments, including lime,[3] clay minerals,[4] biochar,[5] and organic amendments,[6] have proven effective for comprehensive pollution control strategies for Cd-polluted paddy soils. These amendments exhibit varying efficiencies in reducing Cd accumulation in rice grains.[7]

However, chemical immobilization only alters metal speciation rather than removing heavy metals from soil, and soil remediation is a complex and time-consuming process. Consequently, there remains a risk of remobilization or release due to aging processes influenced by various environmental factors,[8] including physical (wet–dry cycles and freeze–thaw events), chemical (*e.g.*, oxidation, soil acidification, and acid precipitation), and biological (*e.g.*, microbial activity)

Key Laboratory of Original Environmental Pollution Control of MARA, Agro-Environmental Protection Institute, Ministry of Agriculture and Rural Affairs, No. 31, Fukang Road, Nankai District, Tianjin 300191, PR China. E-mail: liangxuefeng@caas.cn

† Electronic supplementary information (ESI) available. See DOI: https://doi.org/10.1039/d5em00262a

interactions.[9] Under these environmental conditions, the physicochemical properties of the amendments may change, which, in turn, influences their long-term immobilization effect. Current evaluation criteria predominantly emphasize short-term outcomes, such as crop metal accumulation or soil metal speciation alterations, while insufficient attention has been paid to environmental stability under multifactorial interference or long-term field efficacy.

Environmental stability, or long-term effectiveness, presents a challenge for the practical implementation of immobilization.[10] Direct *in situ* monitoring requires long-term field experiments; therefore, artificial aging has often been employed to simulate aging processes.[11] For instance, atmospheric oxygen and rainwater induce surface oxidation of biochar, resulting in sustained reductions in metal bioavailability following biochar application.[12] Aging decreases the bioavailability of Cu and Cd in biochar-treated soils.[13] A comparative assessment framework revealed that hydroxyapatite and biochar outperform lime in maintaining immobilization efficiency under acid rain conditions.[14] The oxidation of the sulfhydryl group in mercapto-functionalized nanosilica led to a decrease in their ability to immobilize heavy metals.[15] Thus, it is evident that environmental stress may impact the immobilization effect of the amendments.

Among emerging amendments, sulfhydryl grafted palygorskite (SGP) has garnered significant scientific attention. Synthesized through the surface modification of palygorskite with sulfhydryl groups,[16] SGP has been designated as a first-level amendment by the Joint Research Group on Heavy Metal Pollution Remediation of the Ministry of Agriculture and Rural Affairs of China. Numerous studies have validated its efficacy in immobilizing available Cd in alkaline soil,[17] demonstrating success in reducing Cd accumulation in wheat grains through both pot experiments[18] and field-scale applications.[19] SGP could significantly reduce the available Cd content in soil without substantially increasing soil pH at extremely low application doses.[19] This characteristic distinguished it from lime-based pH-regulating amendments, making it particularly suitable for alkaline soils. Furthermore, SGP exhibits superior Cd immobilization selectivity over other trace elements in wheat–rice rotation systems and has shown sustained effectiveness under field conditions.[20] SGP utilizes its sulfhydryl groups to form complexes with Cd as the dominant action mechanism in the sorption of Cd^{2+}.[21] The dose–response relationship of SGP immobilization was nonlinear, and the total amount of sulfhydryl groups added to the soil, rather than the total amount of immobilization amendment, was the key factor determining its immobilization effect.[18]

Despite these advances, the environmental stability and interference resistance of SGP remain inadequately characterized compared with conventional amendments. In this study, the stability of the immobilization effects of SGP on soil-available Cd was investigated at different scales, including exposure to various environmental stresses, simulated rainfall leaching, and temperature interference, and a two-year field-scale demonstration was undertaken. The results and conclusions enhance our understanding of the environmental stability of SGP and provide a theoretical foundation for optimizing management strategies for Cd-contaminated farmland.

2 Materials and methods

2.1 Preparation and characterization of SGP

SGP was synthesized as an immobilization amendment *via* the sol–gel method using colloidal palygorskite and 3-mercaptopropyltrimethoxysilane as precursors.[16] Colloidal palygorskite (Pal), sourced from Xuyi County, Jiangsu Province, exhibited the following primary chemical composition as determined by X-ray fluorescence (XRF, Axios, Panalytical, Netherlands) analysis: SiO_2 (53.7%), MgO (12.3%), Al_2O_3 (7.1%), and H_2O (10.0%). The composition of SGP was SiO_2 (58.83%), SO_3 (17.63%), MgO (5.87%), Al_2O_3 (8.35%), and CaO (2.61%).

The free sulfhydryl content in the SGP sample was quantitatively determined using a colorimetric method[22] after reaction with Ellman's reagent (5,5′-dithiobis(2-nitrobenzoic acid)), using an ultraviolet-visible spectrometer (T700, Persee, China).

Magic-angle spinning ^{29}Si solid-state nuclear magnetic resonance (MAS ^{29}Si NMR) spectra were acquired with an NMR spectrometer (AVANCE NEO, Bruker, Germany) to qualitatively and quantitatively assess sulfhydryl group grafting on Pal. Organic functional surface modifications were analyzed by differential scanning calorimetry (DSC) using a synchronous thermogravimetric differential scanning calorimeter (STA 449F5, Netzsch, Germany) under an N_2 atmosphere at a heating rate of 10 °C min^{-1} (25 to 800 °C). The structural differences between SGP and Pal were characterized by powder X-ray diffraction (XRD) using a powder X-ray diffractometer (D8 Advances, Bruker, Germany). The zeta potentials of SGP and Pal in the pH range of 2–7 were measured using a micro electrophoresis instrument (JS94H, Powereach, China).

2.2 Soil sample analyses

The Cd-contaminated soil samples were collected from the plow layer (0–20 cm) of agricultural fields across multiple provinces. Soils from Xinxiang (abbreviated as XX) and Jiyuan (JY) represented alkaline soil, while Mianzhu (MZ) and Libo (LB) soils were acidic. The soil samples were air-dried, homogenized, manually crushed, and sieved through a 2 mm mesh prior to analysis. Their fundamental properties are listed in Table 1. The total Cd contents in all samples exceeded the risk screening value specified in the Chinese national standard GB 15618-2018 "Soil environmental quality – Risk control standard for soil contamination of agricultural land".

Table 1 Basic physicochemical characteristics of the investigated soil samples

No.	Sampling site	Code	Soil type	pH	Total Cd (mg kg^{-1})
1	Jiyuan, Henan	JY	Cinnamon soil	6.76	2.52
2	Xinxiang, Henan	XX	Fluvo-aquic soil	7.84	2.56
3	Mianzhu, Sichuan	MZ	Paddy soil	5.43	2.39
4	Libo, Guizhou	LB	Paddy soil	5.96	1.58

Soil pH was measured potentiometrically using a pH meter (PHSJ-6L, INESA, China) at a 1 : 2.5 (w/v) soil/water ratio. The total content of heavy metals in the soil was determined *via* digestion with a mixture of HNO_3/HF/$HClO_4$. The soil-available Cd was extracted using a solution containing diethylenetriaminepentaacetic acid (DTPA) (0.005 mol per L DTPA, 0.01 mol per L $CaCl_2$, and 0.1 mol per L triethanolamine at pH 7.3). The concentrations of Cd in the extraction and digestion solutions were quantified using an inductively coupled plasma mass spectrometer (ICP-MS, iCap-Q, Thermo-Fisher, USA). Certified reference material for available nutrients in agricultural soils (GBW07412b) was employed as the control in the analysis.

2.3 Multiple environmental factors interference test

To assess environmental stability, SGP was subjected to the following conditions:

(1) Atmospheric exposure: approximately 10.0 g of SGP was placed in open vessels at 25 °C in an artificial climate chamber (RXM-1008, Jiangnan, China). Each treatment was performed in triplicate. Approximately 1.0 g of SGP sample was collected periodically (1–30 days) for sulfhydryl content analysis and Cd^{2+} sorption capacity testing *via* batch experiments.

(2) Aqueous immersion: approximately 10.0 g of SGP was enclosed in 400-mesh nylon bags and submerged in 500 mL of deionized water at pH 6.8. Each treatment was performed in triplicate. At various sampling time points (0–30 days), approximately 1 g of SGP was separated and dried to analyze the free sulfhydryl content; its Cd sorption amount was determined through batch sorption experiments.

(3) $CuSO_4$ solution: approximately 10.0 g of SGP was placed in 400-mesh nylon bags and submerged in 500 mL of a 10 mg per L $CuSO_4$ solution. The dynamic sampling and subsequent analysis process were the same as the aqueous immersion treatment.

(4) H_2O_2 solution: approximately 10.0 g of SGP was enclosed in 400-mesh nylon bags and submerged in 500 mL of a 0.3% H_2O_2 solution. The dynamic sampling and subsequent analysis process were the same as the aqueous immersion treatment.

(5) Soil environment: approximately 10.0 g of SGP was placed in 400-mesh nylon rhizosphere bags and buried in 500 g of soil samples from JY, XX, MZ, and LB, respectively. At various sampling time points (0–30 days), approximately 1 g of SGP was separated and dried to analyze the free sulfhydryl content, and its Cd sorption amount was determined through batch sorption experiments. Subsequently, the SGP samples were collected and labeled as SGP-JY, SGP-XX, SGP-MZ and SGP-LB. These samples were characterized by X-ray photoelectron spectroscopy (XPS) using a multifunctional imaging electron spectrometer (ESCALAB 250XI, Thermo, USA).

Sorption experiments were conducted to assess the stability of the sulfhydryl content. Approximately 0.5 g of SGP samples after exposure to various environmental stresses were agitated in 500 mL of a $Cd(NO_3)_2$ solution (50 mg per L Cd^{2+}) at 120 rpm for 24 h at 25 °C. The initial and residual Cd^{2+} concentrations were analyzed using ICP-MS to calculate the sorption amounts.

2.4 Simulated rain leaching experiment

The effects of acid rain were evaluated using polypropylene columns (3 cm inner diameter, 25 cm height) filled with contaminated soils (JY, XX, MZ, LB) amended with SGP (0, 0.5, 1.0, 2.0 g kg^{-1}). Simulated rain ($SO_4^{2-}/NO_3^- = 4:1$ molar ratio) was applied at pH 2.6 (acid rain) and 5.6 (natural rain) following the methodology outlined in a previous study.[23] An intermittent leaching procedure was employed, with the simulated rainfall volume calculated based on the leaching solution volume. After filtration through a 0.45 μm filter membrane, the leachate Cd concentration was measured using ICP-MS. The cumulative leaching efficiency of Cd in the soil was calculated as the ratio of the total Cd in the leachates to the total amount of Cd in the soil. Following the leaching experiments, soil pH and available Cd contents were analyzed to assess the stability of SGP immobilization under simulated acid rain conditions.

2.5 Temperature interference and pot experiments

Temperature interference experiments were conducted to investigate the influence of temperature on SGP immobilization efficacy. Soil samples (~500 g) were collected from JY, XX, LB, and MZ and amended with SGP at weight ratios of 0 g kg^{-1} (the control, CK), 0.5 g kg^{-1} (T1), 1.0 g kg^{-1} (T2), and 2.0 g kg^{-1} (T3), with each treatment replicated three times. After a 24 hour equilibrium period, samples were exposed to three temperature conditions based on meteorological data: (1) 25 °C in an artificial climate chamber (RXM-1008, Jiangnan, China), (2) −20 °C in a freezer (BC/BD-519HAN, Haier, China), and (3) 60 °C in a vertical vacuum oven (ZRD-A7230, Zhicheng, China). Samples were maintained at these temperatures and available Cd contents were analyzed after 24, 48, 72 and 96 hours.

Subsequently, all samples were stored at room temperature for a pot experiment conducted in an intelligent greenhouse to assess the stability of the immobilization effects. Pakchoi (*Brassica rapa* var. *chinensis* (L.) Kitam.) was selected as the model plant. Upon harvest, leaf Cd content was determined following HNO_3/$HClO_4$ digestion.

2.6 Field-scale demonstration experiment of crop cultivation

Field-scale demonstrations were conducted in XX and LB to evaluate the stability of the immobilization effect of SGP under actual complex environmental conditions. The field demonstration sites were established in accordance with the national standard "Soil amendments – Regulations of efficiency experiment and assessment" (NY/T 2271-2016). Four different dosages of SGP were applied: 0 g kg^{-1} (CK), 0.5 g kg^{-1}, 1.0 g kg^{-1}, and 2.0 g kg^{-1}. The calculated dosages per unit area were 0.07 kg m^{-2} (T1), 0.14 kg m^{-2} (T2), and 0.28 kg m^{-2} (T3), based on the average depth (20 cm) and average soil density (1.4 g cm^{-3}) of the tillage layer in the local area. SGP was thoroughly mixed with the topsoil in the first year, and no additional amendments were applied in the subsequent year. Each treatment was replicated three times.

In the Libo demonstration, hybrid rice (*Oryza sativa* L. subsp. *indica* Kato) Yexiangyou 959 was selected as the model plant. In

the first year, rice seedlings were transplanted in May, and brown rice was harvested in September. The same procedure was followed in the second year. In the Xinxiang field-scale demonstration, winter wheat (*Triticum aestivum* L.) Bainong 207 was cultivated. Seeds were sown in October of the first year, and wheat grains were harvested in June of the second year. The second growing season began in October and concluded in June of the third year.

Upon harvest, the entire plants and the soil adhering to the roots were collected together. Grain Cd (Cd_{grain}), including Cd contents in wheat grain (Cd_{wheat}) and brown rice (Cd_{rice}), and soil-available Cd (Cd_{DTPA}) were measured following the procedures outlined in the Chinese national standards GB 5009.15-2014 and GB/T 23739-2009. A total of 0.50 g of grain powder was digested using a 10 mL mixed solution of HNO_3/$HClO_4$ (4 : 1, v/v) in an electrothermal digester (DigiBlock ED54, LabTech, China).

2.7 Data processing

Statistical analyses were performed using DPS v20.05 (Data Processing System) with one-way analysis of variance (ANOVA) followed by the Tukey test. Data visualization was generated using OriginPro.

3 Results and discussion

3.1 Structure characterization of SGP

The surface silicon environments were analyzed by ^{29}Si MAS NMR spectroscopy. As illustrated in Fig. 1A, the resonance peak at −89.09 ppm in the Pal spectrum represented the Q^3 site ($Si(OSi)_2(OH)_2$), while the resonance peak at −94.82 ppm corresponded to the Q^4 site ($Si(OSi)_3(OH)$).[24] Additionally, new resonances of T^2 corresponding to ($RSi(OSi)_2(OH)$) and T^3 ($RSi(OSi)_3$) were observed in the SGP spectrum, confirming the successful covalent grafting of sulfhydryl groups onto the palygorskite surface. Furthermore, the peak area of T^3 was significantly larger than that of T^2, indicating that $RSi(OSi)_3$ was the predominant chemical form on the SGP surface.

In the DSC curves presented in Fig. 1B, no significant endothermic or exothermic peaks were detected in the Pal sample within the temperature range of 25–800 °C. However, SGP exhibited a distinct exothermic peak at approximately 340–350 °C, primarily attributed to the decomposition of organic functional groups grafted onto the surface. This exothermic peak provided critical evidence of successful surface modification.

XRD analysis of the patterns in Fig. 1C performed using Jade 6.5, revealed the presence of palygorskite $(Mg,Al)_5(Si,Al)_8O_{20}(OH)_{28}H_2O$ (JCPDS card no. 21-958) and a minor amount of quartz SiO_2 (JCPDS card no. 46-1045) in the Pal sample. For SGP, the characteristic diffraction peak at $2\theta = 8.32°$, corresponding to palygorskite, remained present,[25] albeit with reduced intensity. Overall, the phase composition and structural characteristics of SGP were consistent with those of the original palygorskite, indicating that the sulfhydryl grafting process did not significantly alter the mineral structure.

As shown in Fig. 1D, within the pH range of 2 to 7, the zeta potential of Pal gradually decreased from −10 to 0 mV with

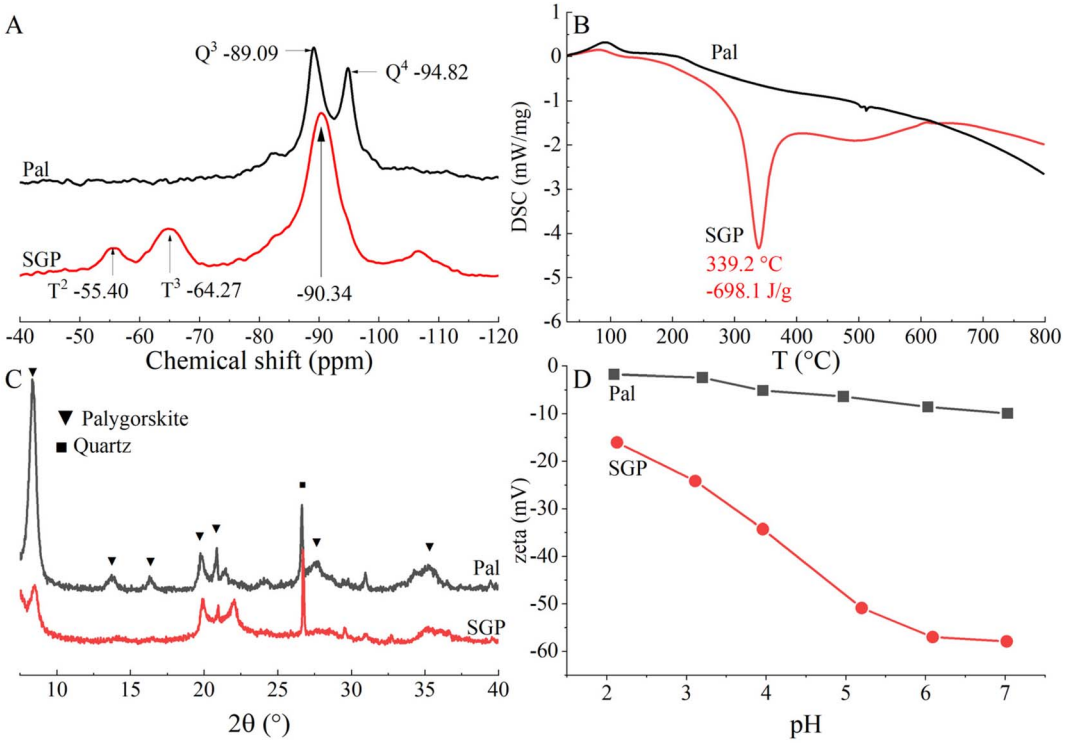

Fig. 1 ^{29}Si NMR spectra, DSC curves, XRD patterns and zeta potentials of SGP and Pal ((A) ^{29}Si MAS NMR spectra; (B) DSC curves; (C) XRD patterns; (D) zeta potentials).

increasing pH. In contrast, SGP exhibited a more pronounced decrease in zeta potential, ranging from −15 to −60 mV over the same pH range. The lower zeta potential observed for SGP, compared with Pal demonstrated that the sulfhydryl groups significantly influenced the surface charge properties, which was advantageous for the sorption and immobilization of heavy metal cations.

3.2 Environmental stability of SGP and its sorption amounts

The free sulfhydryl content of fresh SGP was 2.77 mmol g^{-1}; comparative data under various environmental stresses are presented in Fig. 2. Corresponding arithmetic means and relative standard deviations (RSD) are tabulated in Table S1.† Environmental exposures resulted in sulfhydryl contents ranging from 2.22 to 2.41 mmol g^{-1} (maximum RSD of 3.15%) in the aqueous system and 2.31 to 2.35 mmol g^{-1} (maximum RSD of 3.29%) in soil matrices.

Temporal variations in free sulfhydryl contents of SGP under different environmental stresses are shown in Fig. 3. Atmospheric exposure yielded free sulfhydryl contents between 2.18 and 2.26 mmol g^{-1}, representing a reduction of 18.41% to 21.30% compared with initial values. This reduction exceeded those observed in other media, suggesting that molecular oxygen exerted a significant influence. The oxidation of sulfhydryl groups in air without catalysts was a spontaneous but slow process, primarily occurring through free radical chain reactions to form disulfide bonds.[26] Consequently, long-term storage of SGP in aerobic environments should be avoided.

Immersion in deionized water maintained sulfhydryl contents in the range of 2.31 to 2.41 mmol g^{-1}, with an RSD of 2.95%, demonstrating stability over 30 days. These values substantially exceeded those from atmospheric exposure, confirming that oxygen exclusion mitigated sulfhydryl oxidation. Similar to this study, a sulfhydryl functionalized magnetic covalent organic framework in water, acid and alkali solution environments demonstrated good stability for the quantification of trace heavy metals.[27]

In $CuSO_4$ solution, sulfhydryl contents fluctuated between 2.26 and 2.45 mmol g^{-1} over a 30 day period, representing an 11.55% to 18.41% reduction from the initial values. Despite the chalcophilic properties that facilitate sulfhydryl complexation, the calculated Cu^{2+} concentration (10 mg L^{-1}) accounted for only 2% of SGP's maximum sorption capacity (0.40 mmol g^{-1}).[28] Given that typical soil solution Cu^{2+} levels were orders of magnitude lower than the experimental concentrations, the influence of Cu^{2+} in soil solutions on sulfhydryl groups may be considered negligible.

Exposure to a 0.3% H_2O_2 solution resulted in sulfhydryl contents ranging from 2.25 to 2.36 mmol g^{-1} (RSD of 2.94%). Although proton-mediated oxidation methods (*e.g.*, H_2O_2, HNO_3, H_2SO_4) have conventionally been used to simulate chemical degradation, the necessary peroxidase catalysts for efficient sulfhydryl oxidation were absent in common soil and solution systems.[29] Consequently, SGP demonstrated a relatively stable state in H_2O_2 solution.

Soil-incubated SGP displayed sulfhydryl contents of 2.28–2.51 mmol g^{-1} (JY), 2.24–2.29 mmol g^{-1} (XX), 2.25–2.34 mmol g^{-1} (MZ), and 2.31–2.37 mmol g^{-1} (LB). One-way ANOVA indicated no statistically significant difference in the free sulfhydryl content of SGP samples after 30 days of incubation in either acidic or alkaline soils.

Collectively, free sulfhydryl contents remained stable despite exposure to atmospheric, aqueous, chemical ($CuSO_4$/H_2O_2), and heterogeneous soil environments. This stability suggested that sulfhydryl groups may serve as a structural stability indicator for

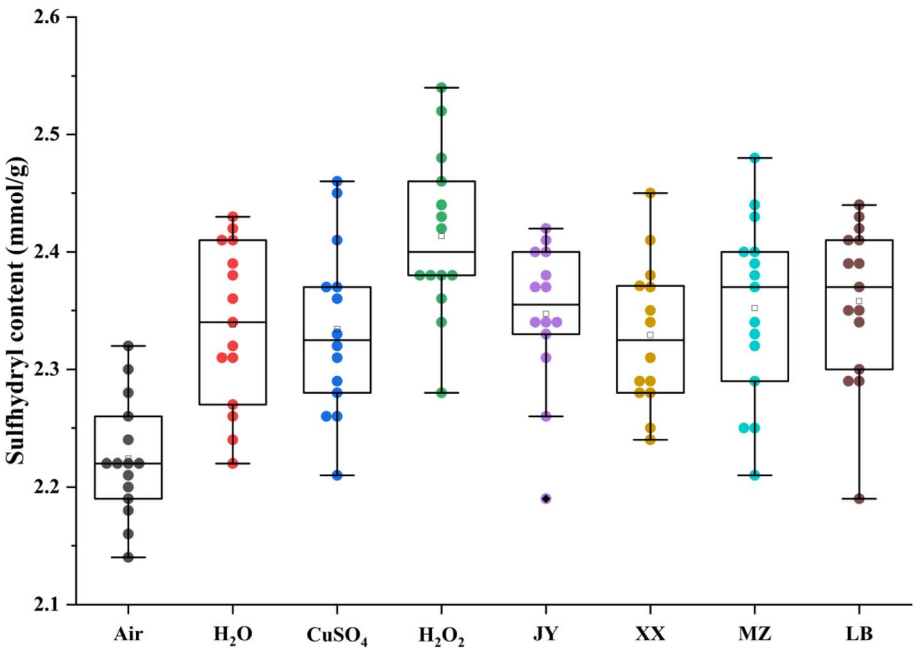

Fig. 2 Free sulfhydryl contents in SGP under environmental stresses.

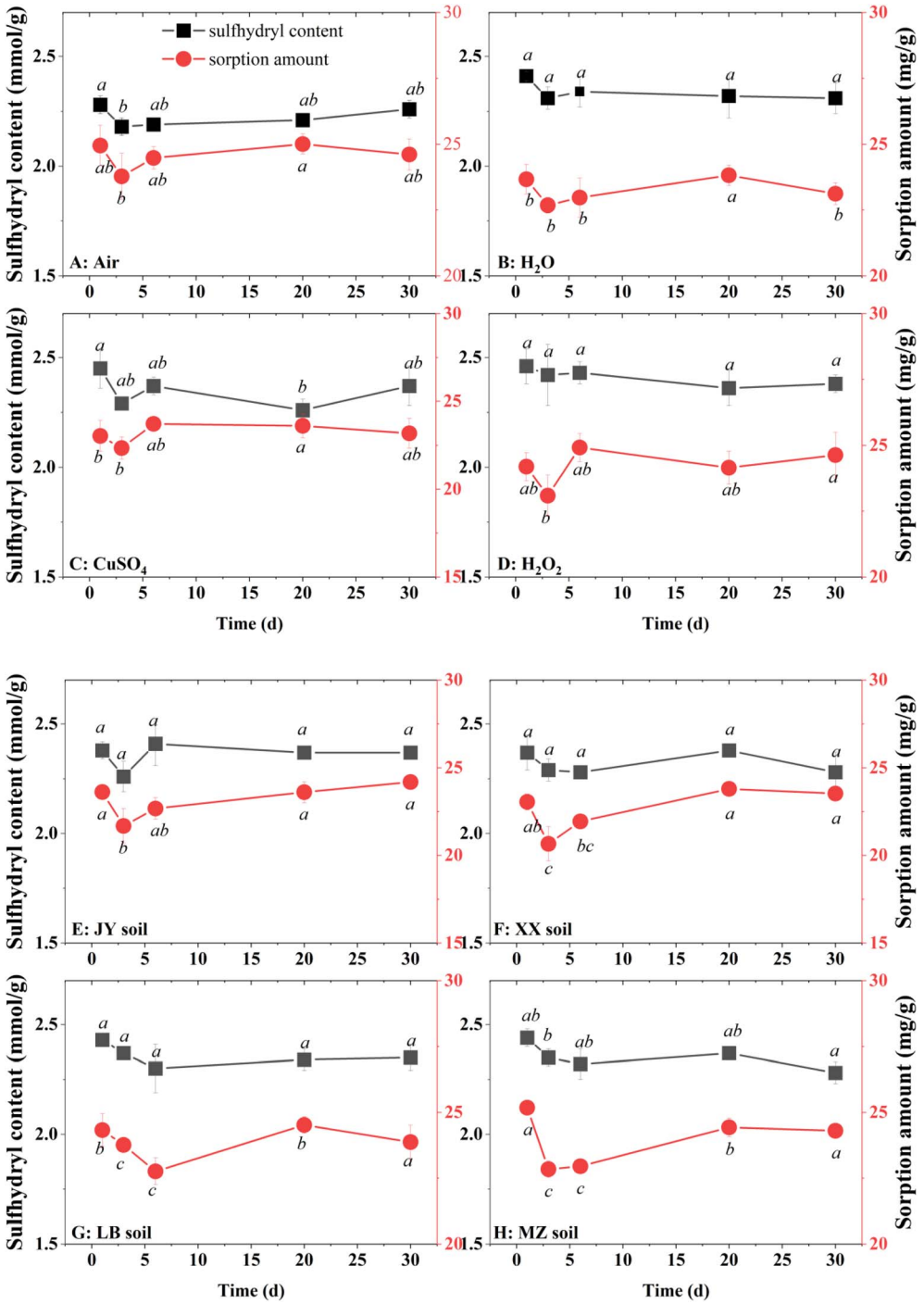

Fig. 3 Sulfhydryl dynamics and Cd sorption in SGP under multifactorial conditions ((A) atmospheric exposure; (B) aqueous immersion; (C) $CuSO_4$ solution; (D) H_2O_2 solution; (E) Jiyuan soil; (F) Xinxiang soil, (G) Libo soil; (H) Mianzhu soil). *Different lowercase letters denote significant differences among sampling times within treatments.

SGP in complex matrices. Subsequent batch sorption experiments revealed that Cd^{2+} sorption amounts (21.68–26.45 mg g^{-1}) correlated positively with sulfhydryl contents, as detailed in Fig. 3.

To further investigate the changes in the properties of SGP under different stress conditions, batch sorption experiments were conducted. A previous study found a positive correlation between the sorption amounts of Cd^{2+} in aqueous solution on SGP and the immobilization ratio in soil environments with the total amounts of free sulfhydryl content in SGP.[18] The dynamics of the saturated sorption amounts of Cd^{2+} on SGP under various environmental stresses over a 30 day period are also presented in Fig. 3. After 30 days of environmental stress, the sorption capacity of SGP did not decrease significantly compared to that

of fresh samples, and its dynamic changes were consistent with the variations in free sulfhydryl content. Thus, the stability of SGP under various environmental stresses could also be assessed from the perspective of sorption capacity.

XPS analysis, as presented in Fig. S1 and Table S2† confirmed that the S 2p binding energy remained at 16.50 eV post-incubation, consistent with sulfhydryl stability. Notably, Cd 3d peaks showed negligible intensity changes, implying minimal Cd^{2+} sorption, attributable to low Cd^{2+} concentrations despite soil contamination. Conversely, Fe 2p and Mn 2p intensities increased by 12–18%, suggesting surface Fe–Mn oxide accumulation.

These findings demonstrate that SGP's structural integrity and sorption functionality remain essentially preserved under various environmental stresses, ensuring long-term effectiveness in heavy metal immobilization.

3.3 Immobilization stability under simulated acid rain leaching

Acid rain has the potential to alter soil properties, modify immobilization amendments, and influence their interactions with heavy metals. The influx of protons (H^+) from acid rain or soil acidification may enhance the bioavailability of Cd in soil,[30] with Cd activation identified as a primary contributor to soil pollution in southern China. The concentrations of Cd^{2+} in leachate from soils amended with SGP were quantified through simulated natural and acid rain leaching, as illustrated in Fig. 4.

Identical Cd^{2+} release patterns were observed in both alkaline and acidic soils, characterized by an exponential decay[31] of leachate Cd^{2+} concentrations with increasing cumulative rainfall, reaching equilibrium at 700 mm. The temporal relationship was mathematically described by the following equation:

$$C_t = (C_0 - C_e)e^{-kV_t} + C_e \quad (1)$$

where C_t represents the instantaneous Cd^{2+} concentration in the soil leachate at time t, C_0 and C_e are the initial and equilibrium leachate Cd^{2+} concentrations, respectively. V_t is the total rainfall calculated from the leaching solution. k is the kinetic constant. The fitted parameters are tabulated in Table 2.

For the Xinxiang soil, the CK group under simulated acid rain treatment exhibited a decrease in leachate Cd concentrations from 4.0 μg L^{-1} to 1.0 μg L^{-1} at 700 mm rainfall. The T1 treatment group showed a reduction from 1.9 μg L^{-1} to 0.5 μg L^{-1}. According to the national standard for groundwater quality GB/T 14848-2017, the maximum permissible Cd concentrations for class III and class II groundwater are 5 μg L^{-1} and 1 μg L^{-1}, respectively. During the initial leaching stages, leachates from the CK group exceeded class III limits, while SGP-amended groups complied with the class II standard throughout the leaching experiment. These results demonstrated the effectiveness of SGP in controlling soil Cd availability and maintaining stability under acid rain conditions.

SGP-amended groups exhibited significantly lower leachate Cd concentrations compared with the CK groups, particularly during the initial leaching phases (0–200 mm of rainfall). This marked reduction confirmed the capacity of SGP to immobilize available Cd. The sustained low Cd concentrations under acid rain leaching further indicated robust stabilization performance against acidic perturbations.

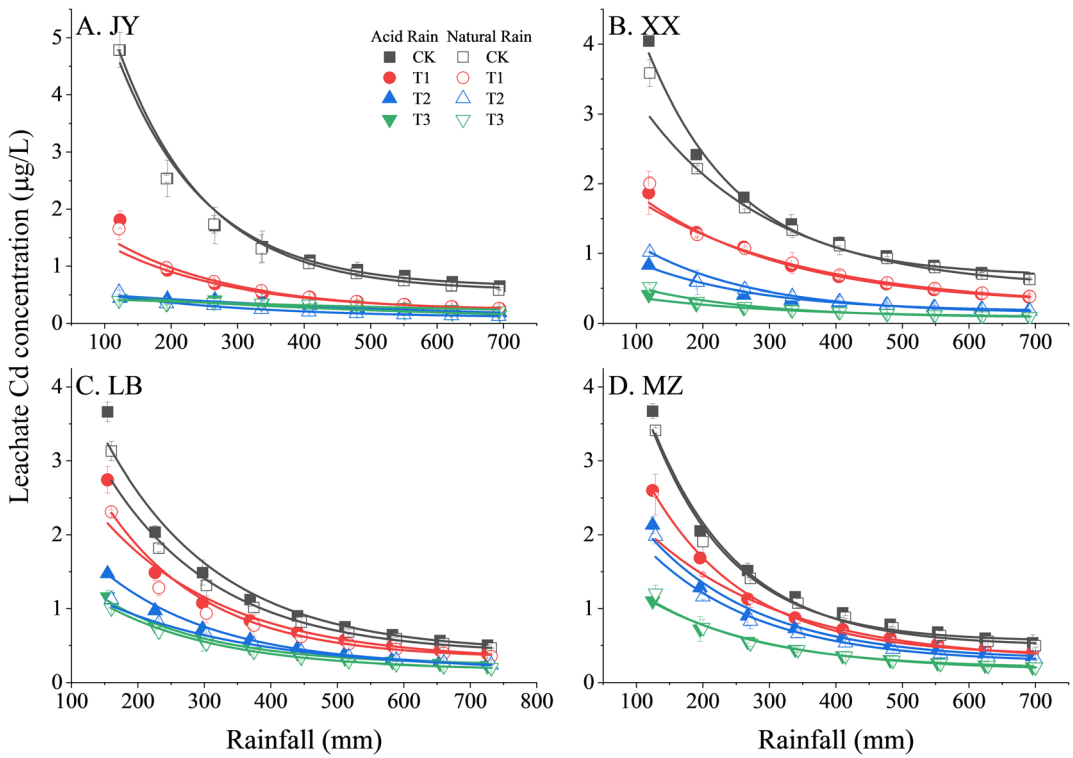

Fig. 4 Dynamic changes of the leachate Cd in different soils under simulated rainfall ((A–D): Jiyuan, Xinxiang, Libo, Mianzhu soils).

Table 2 Regression parameters characterizing the relationship between leachate Cd^{2+} and cumulative rainfall

		Acid rain				Natural rain			
Soil	Parameter	CK	T1	T2	T3	CK	T1	T2	T3
JY	C_0 (μg L^{-1})	10.48 ± 1.24	2.25 ± 0.35	0.59 ± 0.054	0.58 ± 0.086	11.17 ± 0.26	2.51 ± 0.25	0.72 ± 0.088	0.46 ± 0.052
	C_e (μg L^{-1})	0.63 ± 0.028	0.23 ± 0.019	0.01 ± 0.18	0.01 ± 0.12	0.57 ± 0.029	0.22 ± 0.012	0.093 ± 0.021	0.01 ± 0.63
	k	0.0075 ± 6.6 × 10^{-4}	0.0055 ± 6.9 × 10^{-4}	0.0016 ± 0.0010	0.0018 ± 9.9 × 10^{-4}	0.0076 ± 2.2 × 10^{-4}	0.0055 ± 3.9 × 10^{-4}	0.0042 ± 7.5 × 10^{-4}	9.28 × 10^{-4} ± 0.0018
	R^2	0.9742	0.9815	0.9761	0.9465	0.9994	0.9931	0.9777	0.8596
XX	C_0 (μg L^{-1})	8.26 ± 0.69	2.76 ± 0.14	1.40 ± 0.10	0.54 ± 0.081	5.03 ± 0.46	2.55 ± 0.27	1.90 ± 0.066	0.85 ± 0.098
	C_e (μg L^{-1})	0.68 ± 0.029	0.27 ± 0.014	0.17 ± 0.021	0.085 ± 0.011	0.49 ± 0.035	0.2472 ± 0.10	0.15 ± 0.0065	0.082 ± 0.0068
	k	0.0073 ± 4.3 × 10^{-4}	0.0045 ± 2.2 × 10^{-4}	0.0056 ± 6.0 × 10^{-4}	0.0045 ± 8.9 × 10^{-4}	0.0051 ± 4.8 × 10^{-4}	0.0040 ± 7.9 × 10^{-4}	0.0058 ± 3.4 × 10^{-4}	0.0056 ± 6.0 × 10^{-4}
	R^2	0.9964	0.9997	0.9978	0.9847	0.9946	0.9869	0.9999	0.9768
LB	C_0 (μg L^{-1})	7.36 ± 0.84	4.52 ± 0.65	3.24 ± 0.14	2.47 ± 0.27	6.47 ± 0.59	5.98 ± 0.29	1.92 ± 0.025	2.22 ± 0.045
	C_e (μg L^{-1})	0.41 ± 0.025	0.30 ± 0.020	0.21 ± 0.012	0.24 ± 0.032	0.39 ± 0.014	0.33 ± 0.015	0.17 ± 0.0028	0.17 ± 0.0039
	k	0.0058 ± 3.6 × 10^{-4}	0.0053 ± 4.5 × 10^{-4}	0.0057 ± 2.7 × 10^{-4}	0.0061 ± 7.4 × 10^{-4}	0.0060 ± 2.8 × 10^{-4}	0.0066 ± 2.9 × 10^{-4}	0.00437 ± 6.9 × 10^{-5}	0.0056 ± 1.3 × 10^{-4}
	R^2	0.9788	0.9749	0.9973	0.9881	0.9950	0.9970	0.9999	0.9996
MZ	C_0 (μg L^{-1})	8.35 ± 1.27	5.64 ± 0.14	3.74 ± 0.37	2.08 ± 0.032	8.10 ± 0.59	3.36 ± 0.14	3.31 ± 0.29	1.98 ± 0.20
	C_e (μg L^{-1})	0.55 ± 0.030	0.37 ± 0.0047	0.30 ± 0.018	0.19 ± 0.0064	0.49 ± 0.017	0.28 ± 0.011	0.27 ± 0.018	0.17 ± 0.0051
	k	0.0081 ± 9.4 × 10^{-4}	0.0069 ± 1.9 × 10^{-4}	0.0060 ± 4.6 × 10^{-4}	0.0059 ± 1.5 × 10^{-4}	0.0076 ± 4.3 × 10^{-4}	0.0048 ± 1.6 × 10^{-4}	0.0058 ± 4.1 × 10^{-4}	0.0055 ± 3.3 × 10^{-4}
	R^2	0.9848	0.9995	0.9828	0.9997	0.9928	0.9968	0.9871	0.9985

Under both acid and natural rain leaching, total Cd leaching ratios exhibited increasing trends with rainfall intensity (Fig. 5). The first- and second-order kinetic equations (eqn (2) and (3)) were employed to fit the leaching data.[32] The relationship between leaching efficiency (LE) and rainfall was successfully modeled using first-order kinetics, and the corresponding fitting parameters are listed in Table 3.

$$LE_t = LE_{m1}(1 - e^{-k_1 V_t}) \quad (2)$$

$$LE_t = \frac{k_2 LE_{m2}{}^2}{1 + k_2 LE_{m2} V_t} \quad (3)$$

LE_t is the leaching efficiency at the rainfall of V_t, LE_{m1} and LE_{m2} are the maximum leaching efficiency at the equilibrium stage fitted by the first- and second-order kinetic equations, and k_1 and k_2 correspond to the kinetic constants.

The second-order kinetic equation demonstrated superior fitting for the leaching process, consistent with the immobilization of heavy metals by goethite-loaded montmorillonite in non-ferrous metal smelting areas.[33] In the second-order kinetic equation, k_2 represents the reciprocal of the maximum release,[34] while LE_{m2} denotes the maximum release amounts. As shown in Table 3, LE_{m2} values in SGP-amended soils were lower than those in the control, whereas k_2 exhibited an inverse relationship trend with LE_{m2}, indicating stable immobilization under acid rain stress.

Unamended soils displayed rapid Cd release during the initial leaching phase (0–200 mm rainfall), attributed to the dissolution of surface-adsorbed Cd particles, consistent with acid rain leaching characteristics observed in mine tailings.[35] In contrast, SGP-amended soils maintained consistent leaching efficiency throughout the experiments, with Cd release inversely proportional to the amendment dosage. For Mianzhu soil, control groups exhibited total Cd leaching efficiencies of 0.89% (acid rain) and 0.83% (natural rain) at 700 mm rainfall. SGP treatment (T3) reduced these values to 0.32% and 0.31%, respectively. Kinetic modeling predicted a leaching efficiency of 0.41% under 2000 mm rainfall, twice the average annual precipitation, confirming the long-term immobilization stability of SGP under prolonged acid rain exposure.

While leachate Cd concentrations and leaching ratios provided indirect evidence of immobilization effects, direct confirmation was obtained from the available Cd concentrations in soil columns post-leaching.[33] As illustrated in Fig. S2,† SGP reduced available Cd by 63.2–84.2% in Jiyuan soil, 47.7–78.8% in Xinxiang soil, 73.7–94.7% in Libo soil, and 63.2–88.9% in Mianzhu soil following acid rain leaching. Notably, soil pH remained stable in SGP-treated groups post-leaching, consistent with previous findings demonstrating acid rain resistance in mercapto-functionalized palygorskite at 1–3% application rates.[36] This stability further corroborated the structural integrity of SGP under acidic conditions.

3.4 Impact of temperature variations on SGP immobilization efficacy

The available Cd contents in Jiyuan, Xinxiang, Mianzhu, and Libo soils exhibited minimal fluctuations (RSD < 5%) across

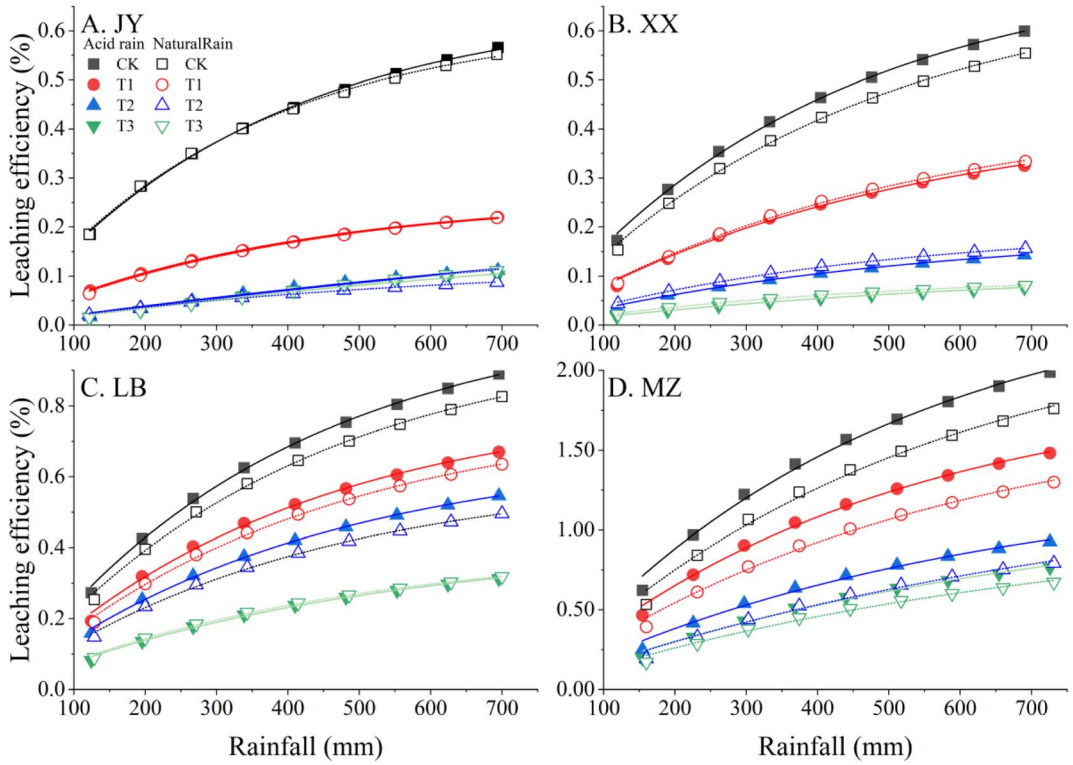

Fig. 5 Leaching efficiency by simulated rain in SGP amended soils ((A–D): Jiyuan, Xinxiang, Libo, Mianzhu soils).

temperature regimes (−20 °C, 25 °C, and 60 °C) during the 0–96 h exposure period, as demonstrated in Fig. 6A–D.

In Jiyuan soil, control samples maintained available Cd contents of 1.63–1.87 mg kg^{-1} (mean: 1.77 mg kg^{-1}) under cryogenic conditions (−20 °C). SGP amendment induced significant reductions in available Cd, achieving decrement percentages of 65.03%, 68.75%, and 73.22% across treatment groups (T1–T3) after 96 h. Similar stabilization patterns were observed under 60 °C thermal stress, consistent with the findings from −20 °C freezing conditions. Maximum Cd immobilization efficiencies of 63.67% (T1), 80.13% (T2), and 89.83% (T3) were recorded, confirming temperature-independent remediation performance. Acidic soils (Mianzhu/Libo) demonstrated rapid efficacy, with T1 treatment yielding 43.61%, 52.56%, and 55.02% reduction in available Cd after 24 h exposure to −20 °C, 25 °C, and 60 °C, respectively. Consistent with the findings of this study, freeze–thaw temperature variations did not significantly alter the bioavailability of Cd in biochar-amended soil,[13] and the immobilization efficiencies of mercapto iron functionalized nanosilica for Cd and Pb bioavailability remained stable across a wide temperature range (−20 to 50 °C).[15]

Following the pot experiment involving soil pretreated at various temperatures, the soil-available Cd contents are presented in Fig. S3.† Consistent with the findings from the dynamic sampling analysis, SGP demonstrated significant immobilization effects across all three dosages, with the pretreatment temperature exhibiting no substantial influence on the immobilization efficacy of SGP. Phytotoxicity assessments conducted using pakchoi revealed that the immobilization efficacy was independent of temperature (Fig. S4†). In CK groups of Jiyuan soil, the leaf Cd contents ranged from 0.85 to 1.01 mg kg^{-1}, exceeding the threshold (0.20 mg kg^{-1}) established by the China National Standard GB 2762-2022 and the international standard Codex Stan 193-1995 proposed by the Food and Agriculture Organization of the United Nations. The application of SGP amendment resulted in a dose-dependent reduction in leaf Cd content, achieving levels of 0.39 mg kg^{-1} (T1, 59.9% reduction), 0.25 mg kg^{-1} (T2, 73.8% reduction), and 0.15 mg kg^{-1} (T3, 84.9% reduction) at 25 °C.

For the soil samples subjected to −20 °C and 60 °C pretreatment, the leaf Cd contents in the T1, T2, and T3 were in the range of 0.35 to 0.40 mg kg^{-1}, 0.20 to 0.26 mg kg^{-1}, and 0.08 to 0.16 mg kg^{-1}, respectively. Notably, T3-treated samples complied with the GB 2762-2022 standard, irrespective of thermal pretreatment. Compared with the 25 °C treatment, the continuous −20 °C and 60 °C pretreatments did not significantly promote or inhibit leaf Cd contents, indicating that the immobilization effect of SGP was minimally affected by temperature changes.

The Xinxiang soil controls exhibited elevated leaf Cd concentrations (1.01–1.14 mg kg^{-1}), which were mitigated by SGP to 0.44–0.58 mg kg^{-1} for T1, 0.30–0.40 mg kg^{-1} for T2 and 0.16–0.19 mg kg^{-1} for T3. Statistical analysis confirmed no significant temperature-dependent differences within dosage groups, underscoring the thermal resilience of SGP.

For the acidic soils from Mianzhu and Libo, the trends observed in the control group and SGP treatment group were

Table 3 Kinetic parameters quantifying the dynamic correlation between Cd leaching efficiency and rainfall intensity

			Simulated acid rain				Simulated natural rain			
	Soil	Parameter	CK	T1	T2	T3	CK	T1	T2	T3
First-order kinetics	JY	LE_{m1}	0.65 ± 0.0093	0.26 ± 0.0030	0.32 ± 0.10	0.25 ± 0.068	0.62 ± 0.0079	0.27 ± 0.0051	0.13 ± 0.0055	0.15 ± 0.031
		k_1	0.0028 ± 8.2 × 10^{-5}	0.0026 ± 5.9 × 10^{-5}	$6.3 \times 10^{-4} \pm 2.5 \times 10^{-4}$	$7.7 \times 10^{-4} \pm 2.6 \times 10^{-4}$	0.0031 ± 8.4 × 10^{-5}	0.0025 ± 8.8 × 10^{-5}	0.0017 ± 1.2 × 10^{-4}	$8.7 \times 10^{-5} \pm 1.9 \times 10^{-4}$
		R^2	0.9984	0.9992	0.9870	0.9855	0.9984	0.9982	0.9969	0.9917
	XX	LE_{m1}	0.73 ± 0.013	0.44 ± 0.019	0.19 ± 0.0062	0.12 ± 0.0047	0.70 ± 0.015	0.45 ± 0.015	0.20 ± 0.0039	0.10 ± 0.0019
		k_1	0.0025 ± 8.4 × 10^{-5}	0.0020 ± 1.5 × 10^{-4}	0.0019 ± 1.0 × 10^{-4}	0.0015 ± 9.2 × 10^{-5}	0.0023 ± 8.9 × 10^{-5}	0.0020 ± 1.2 × 10^{-4}	0.0022 ± 7.7 × 10^{-5}	0.0022 ± 6.8 × 10^{-5}
		R^2	0.9984	0.9953	0.9976	0.9981	0.9982	0.9969	0.9987	0.9989
	LB	LE_{m1}	2.55 ± 0.11	1.91 ± 0.073	1.33 ± 0.10	1.18 ± 0.10	2.37 ± 0.13	1.78 ± 0.089	1.34 ± 0.17	1.07 ± 0.11
		k_1	0.0021 ± 1.6 × 10^{-4}	0.0021 ± 1.4 × 10^{-4}	0.0017 ± 2.1 × 10^{-4}	0.0015 ± 1.9 × 10^{-4}	0.0019 ± 1.7 × 10^{-4}	0.0018 ± 1.5 × 10^{-4}	0.0013 ± 2.3 × 10^{-4}	0.0014 ± 2.1 × 10^{-4}
		R^2	0.9927	0.9942	0.9882	0.9897	0.9909	0.9931	0.9849	0.9870
	MZ	LE_{m1}	1.06 ± 0.018	0.82 ± 0.022	0.68 ± 0.014	0.42 ± 0.015	1.00 ± 0.019	0.79 ± 0.018	0.61 ± 0.014	0.41 ± 0.011
		k_1	0.0026 ± 8.5 × 10^{-5}	0.0025 ± 1.3 × 10^{-4}	0.0024 ± 9.1 × 10^{-5}	0.0020 ± 1.2 × 10^{-4}	0.0025 ± 9.4 × 10^{-5}	0.0024 ± 1.0 × 10^{-4}	0.0024 ± 1.0 × 10^{-4}	0.0022 ± 1.1 × 10^{-4}
		R^2	0.9983	0.9962	0.9980	0.9966	0.9978	0.9975	0.9975	0.9971
Second-order kinetics	JY	LE_{m2}	0.95 ± 0.022	0.38 ± 0.0075	0.60 ± 0.23	0.46 ± 0.15	0.89 ± 0.023	0.40 ± 0.015	0.20 ± 0.014	0.18 ± 0.012
		k_2	0.0023 ± 1.6 × 10^{-4}	0.005 ± 2.8 × 10^{-4}	$5.6 \times 10^{-4} \pm 4.6 \times 10^{-4}$	$9.2 \times 10^{-4} \pm 6.6 \times 10^{-4}$	0.0027 ± 2.1 × 10^{-4}	0.0044 ± 4.7 × 10^{-4}	0.0053 ± 8.9 × 10^{-4}	0.0081 ± 5.1 × 10^{-5}
		R^2	0.9980	0.9988	0.9867	0.9849	0.9970	0.9965	0.9957	0.9917
	XX	LE_{m2}	1.10 ± 0.040	0.69 ± 0.048	0.31 ± 0.015	0.19 ± 0.012	1.07 ± 0.044	0.70 ± 0.041	0.31 ± 0.012	0.16 ± 0.0056
		k_2	0.0016 ± 1.7 × 10^{-4}	0.0019 ± 3.6 × 10^{-4}	0.0042 ± 5.5 × 10^{-4}	0.0050 ± 7.4 × 10^{-4}	0.0015 ± 1.7 × 10^{-4}	0.0019 ± 2.9 × 10^{-4}	0.0050 ± 5.4 × 10^{-4}	0.0093 ± 8.7 × 10^{-4}
		R^2	0.9967	0.9932	0.9967	0.9973	0.9966	0.9951	0.9971	0.9978
	LB	LE_{m2}	3.92 ± 0.27	2.94 ± 0.19	2.14 ± 0.24	1.96 ± 0.24	3.71 ± 0.31	2.81 ± 0.22	2.27 ± 0.38	1.79 ± 0.25
		k_2	$3.7 \times 10^{-4} \pm 7.1 \times 10^{-5}$	$4.9 \times 10^{-4} \pm 8.6 \times 10^{-5}$	$5.1 \times 10^{-4} \pm 1.4 \times 10^{-4}$	$4.7 \times 10^{-4} \pm 1.4 \times 10^{-4}$	$3.4 \times 10^{-4} \pm 7.7 \times 10^{-5}$	$4.3 \times 10^{-4} \pm 8.8 \times 10^{-5}$	$3.4 \times 10^{-4} \pm 1.4 \times 10^{-4}$	$4.8 \times 10^{-4} \pm 1.6 \times 10^{-4}$
		R^2	0.9896	0.9915	0.9855	0.9878	0.9880	0.9907	0.9832	0.9850
	MZ	LE_{m2}	1.58 ± 0.055	1.22 ± 0.059	1.02 ± 0.040	0.65 ± 0.038	1.50 ± 0.059	1.19 ± 0.052	0.92 ± 0.040	0.63 ± 0.031
		k_2	0.0012 ± 1.2 × 10^{-4}	0.0015 ± 2.0 × 10^{-4}	0.0016 ± 1.8 × 10^{-4}	0.0021 ± 3.2 × 10^{-4}	0.0012 ± 1.3 × 10^{-4}	0.0014 ± 1.7 × 10^{-4}	0.0018 ± 2.2 × 10^{-4}	0.0024 ± 3.2 × 10^{-4}
		R^2	0.9965	0.9939	0.9965	0.9948	0.9959	0.9954	0.9955	0.9953

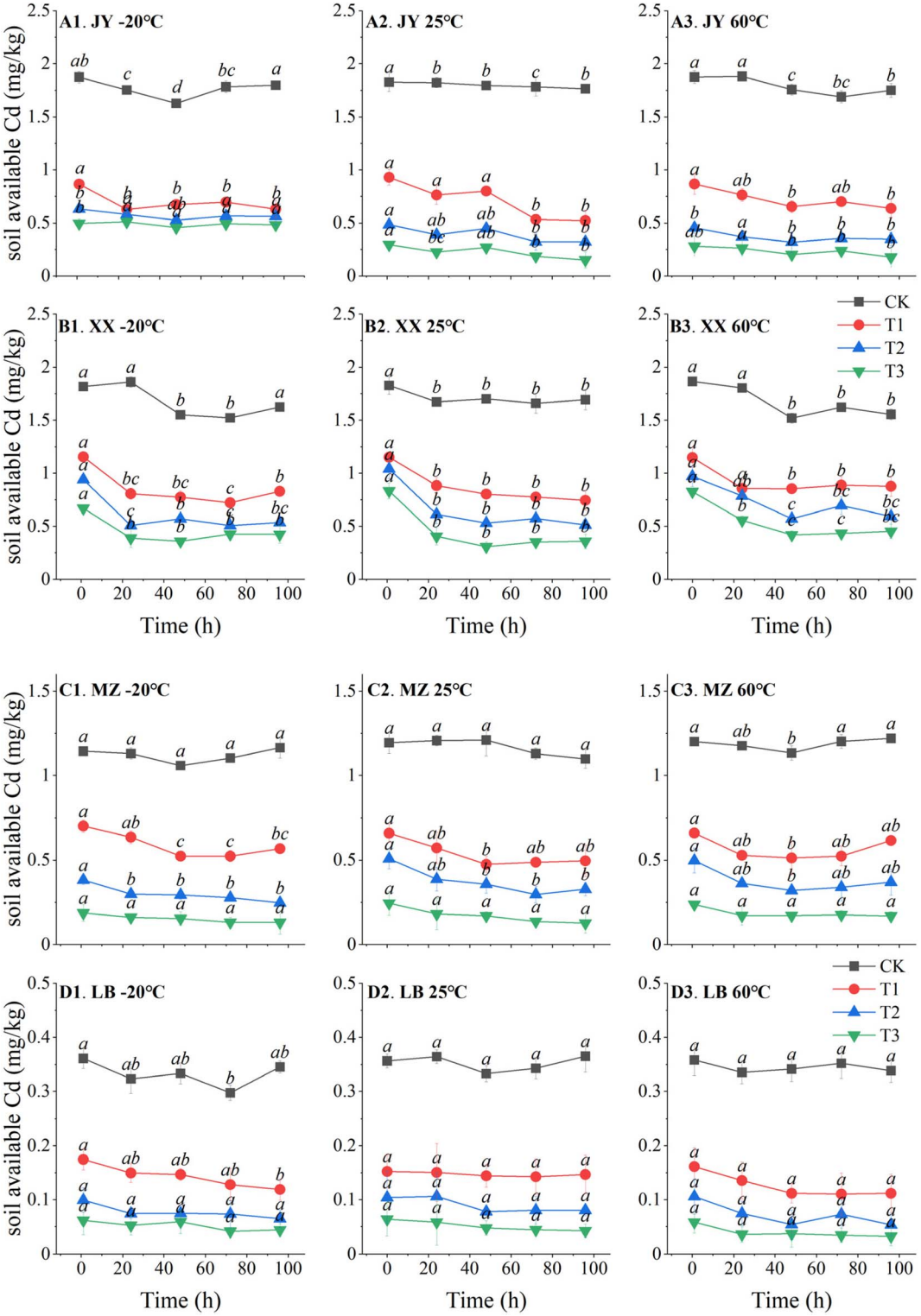

Fig. 6 Available Cd dynamics in SGP amended soils under different temperatures ((A–D): Jiyuan, Xixiang, Mianzhu, Libo soils; 1–3: −20 °C, 25 °C, 60 °C). The different lowercase letters above the data point indicate statistical differences between different sampling times for the same treatment.

similar to those of the alkaline soil group. At the same temperature pretreatment, significant differences were observed among the different dosages of SGP. It was noted that the dosages of SGP exhibited a negative correlation with leaf Cd contents. Under the same dosage of SGP, no significant differences were observed among different temperature

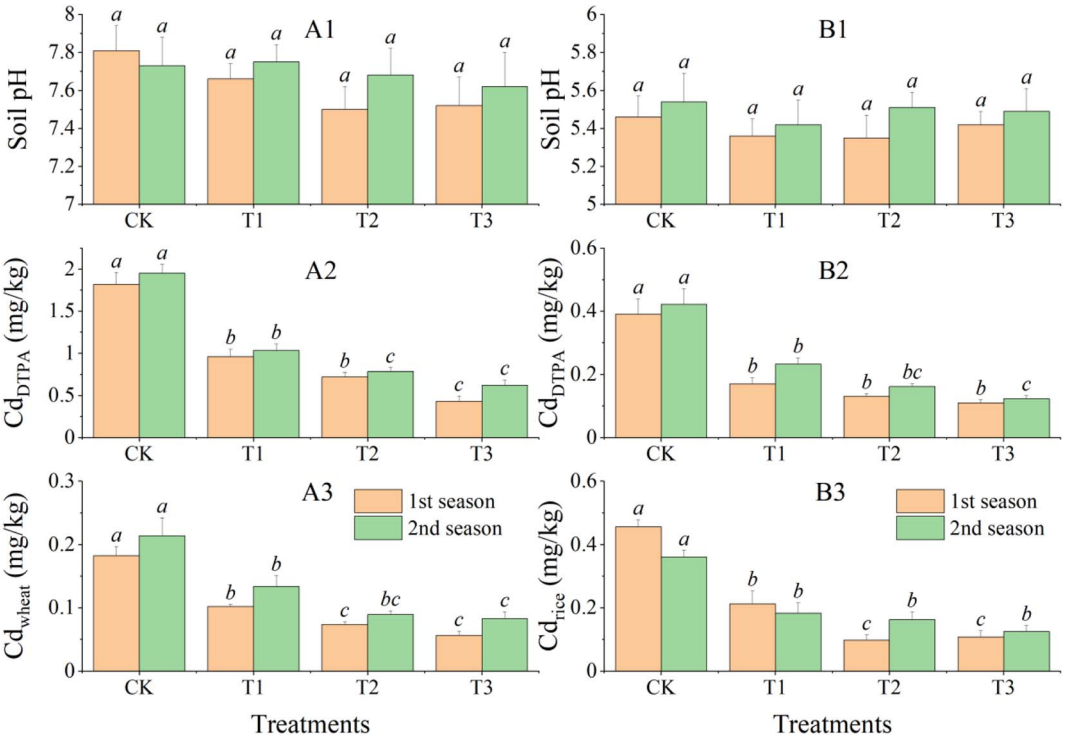

Fig. 7 Soil pH, Cd availability and grain accumulation in field-scale demonstration in Xinxiang and Libo in two consecutive seasons ((A1–A3) soil pH values, soil available Cd contents and wheat grain Cd contents in Xinxiang field demonstration; (B1–B3) soil pH values, soil available Cd contents and rice grain Cd contents in Libo field demonstration). *The different lowercase letters above the data column indicate statistical differences between the different immobilization treatments in the same growing season.

pretreatments. This result is consistent with previous findings: soil-available Cd was not affected by temperature changes during freeze–thaw cycles, and the amendment calcined rectorite demonstrated high stability.[37]

3.5 Universal stability of immobilization effects in field-scale demonstration

Although the stability of SGP could be preliminarily assessed by simulating environmental stresses, field demonstrations remain the most reliable method for evaluating the actual effectiveness of immobilization amendments. Therefore, this study selected typical acidic and agricultural soils for two consecutive years of field demonstrations to examine the stability of SGP under natural conditions. As illustrated in Fig. 7A1, the pH values of alkaline Xinxiang soil in control groups (CK) remained stable at 7.81 and 7.83 during the first and second growing seasons, respectively. The SGP amendment induced marginal pH reductions to 7.50–7.66 (first year) and 7.62–7.75 (second year), with no statistically significant differences compared with CK. This pH stability aligns with previous studies demonstrating SGP's neutral impact on soil acidity.[38] Acidic Libo soil exhibited analogous behavior (Fig. 7B1), further confirming that SGP exerted neither promotive nor inhibitory effects on soil acidity, a significant feature that distinguishes SGP from other pH-regulating amendments, such as biochar.[39]

Soil-available Cd contents in Xinxiang CK groups measured 1.82 and 1.95 mg kg^{-1} across consecutive years (Fig. 7A2). SGP treatments effectively reduced these values to 0.43–0.96 mg kg^{-1} (first year) and 0.62–1.03 mg kg^{-1} (second year), corresponding to immobilization ratios of 47.3–76.4% and 47.2–68.2%, respectively. Mercapto functionalized palygorskite could promote the transformation of free Fe/Mn oxides into amorphous oxides, and enhance the immobilization of Cd in alkaline soil.[40]

In the Libo field demonstration, SGP achieved comparable performance (Fig. 7B2), with Cd immobilization ratios of 56.4–71.8% (the first year) and 45.2–71.4% (the second year).

Grain Cd contents served as the critical endpoint for immobilization efficacy assessment. In the Xinxiang trials (Fig. 7A3), CK wheat grain contained 0.18 mg kg^{-1} (first year) and 0.21 mg kg^{-1} (second year) Cd. SGP treatments reduced these values to 0.06–0.10 mg kg^{-1} in the first year (44.4–66.7% reduction) and 0.08–0.13 mg kg^{-1} in the second year (38.1–61.9% reduction). The results are consistent with the reported immobilization efficiency of mercapto palygorskite on DTPA extractable Cd under field conditions.[19] The Libo field results (Fig. 7B3) revealed control brown rice Cd contents of 0.46 and 0.36 mg kg^{-1}, both exceeding national food safety thresholds (GB 2762-2022). SGP amendments suppressed rice grain Cd accumulation to 0.10–0.21 mg kg^{-1} (54.3–78.3% reduction) and 0.12–0.18 mg kg^{-1} (50.0–66.7% reduction) across seasons. Statistical analysis confirmed no interannual differences in soil available Cd or grain Cd contents.

Thiol-modified biochar exhibited long-term efficacy in reducing mercury mobility and associated health risks in soil over a two-year period.[41] MPTS/nano-silica effectively reduced

the leachability and bioavailability of soil Cd, exhibiting persistent stabilization effects under field conditions for three years.[42]

Strong linear correlations between soil available Cd and grain Cd contents confirmed the consistent performance of SGP. The sustained immobilization efficacy observed over two consecutive growing seasons in contrasting soil types (acidic and alkaline) validated the environmental stability of SGP-mediated Cd immobilization mechanisms under field conditions.

4 Conclusion

SGP demonstrated chemical stability across diverse media, including ambient atmosphere, aqueous solution and heterogeneous soil matrices. Quantitative verification through free sulfhydryl group retention and consistent heavy metal sorption capacity under environmental stress confirmed this intrinsic stability. Furthermore, SGP demonstrated significant resilience to key environmental stresses. Simulated acid rain leaching experiments revealed no statistically significant impact on Cd^{2+} mobilization from SGP amended soils, confirming the amendment's resistance to acidic precipitation. Thermal variance further demonstrated the temperature-insensitive performance characteristics, with less than 10% fluctuation observed in both soil available Cd regulation and Cd uptake by pakchoi. Field validation in contrasting pedological systems (acidic *vs.* alkaline soils) established universal immobilization stability, maintaining reductions in soil-available Cd and grain Cd content across seasonal variations.

This systematic investigation employing comprehensive qualitative and quantitative characterization provides fundamental criteria for evaluating SGP stability. It achieved two critical advancements: providing mechanistic validation for large-scale SGP implementation in contaminated farmland remediation and developing standardized protocols for novel amendment stability assessment.

Data availability

Data will be made available upon request.

Author contributions

Miao Wang: investigation, writing – original draft. Xusheng Gao: investigation. Xilin Chen: software, methodology. Yifei Shu: data curation. Qingqing Huang: methodology, investigation. Lin Wang: visualization, investigation. Xu Qin: validation, formal analysis. Yuebing Sun: supervision, project administration. Yujie Zhao: investigation, validation. Xuefeng Liang: conceptualization, reviewing, revising.

Conflicts of interest

This work has not been published previously, in whole or in part, and not under consideration for publication elsewhere. All the authors listed have approved the manuscript that is enclosed. All the authors declare no conflict of interest, either financial or otherwise.

Acknowledgements

The current research was supported by the National Key Research and Development Program of China (2024YFD1701103) and the Innovation Program of the Chinese Academy of Agricultural Sciences.

References

1 T. Shi, Y. Zhang, Y. Gong, J. Ma, H. Wei, X. Wu, L. Zhao and H. Hou, Status of cadmium accumulation in agricultural soils across China (1975–2016): From temporal and spatial variations to risk assessment, *Chemosphere*, 2019, **230**, 136–143.

2 F. S. Mabagala, T. Zhang, X. Zeng, C. He, H. Shan, C. Qiu, X. Gao, N. Zhang and S. Su, A review of amendments for simultaneously reducing Cd and As availability in paddy soils and rice grain based on meta-analysis, *J. Environ. Manage.*, 2024, **366**, 121661.

3 L. Kong, Z. Guo, C. Peng, X. Xiao and Y. He, Factors influencing the effectiveness of liming on cadmium reduction in rice: A meta-analysis and decision tree analysis, *Sci. Total Environ.*, 2021, **779**, 146477.

4 Y. Hamid, L. Tang, B. Hussain, M. Usman, L. Liu, Z. Ulhassan, Z. He and X. Yang, Sepiolite clay: A review of its applications to immobilize toxic metals in contaminated soils and its implications in soil–plant system, *Environ. Technol. Innovation*, 2021, **23**, 101598.

5 Z. Yan, W. Ding, G. Xie, M. Yan and Q. Wang, Limiting the mobility and phytoavailability of cadmium in paddy-upland soils after the application of various biochar fractions and proportions, *Ecotoxicol. Environ. Saf.*, 2025, **295**, 118124.

6 X. Wei, H. Tian, H. Yan, G. He, L. Mou, T. Fu, X. Li, C. Huang, R. Cen, Z. Zhong, T. He and S. Yang, Organic and inorganic amendments under flooded irrigation reduce Cd bioavailability and its uptake by rice in Cd-contaminated soil, *Environ. Technol. Innovation*, 2024, **36**, 103879.

7 J. Gao, H. Han, C. Gao, Y. Wang, B. Dong and Z. Xu, Organic amendments for in situ immobilization of heavy metals in soil: A review, *Chemosphere*, 2023, **335**, 139088.

8 C. Peng, K. Gong, Q. Li, W. Liang, H. Song, F. Liu, J. Yang and W. Zhang, Simultaneous immobilization of arsenic, lead, and cadmium in soil by magnesium-aluminum modified biochar: Influences of organic acids, aging, and rainfall, *Chemosphere*, 2023, **313**, 137453.

9 X. Li, L. Wang and D. Hou, Layered double hydroxides for simultaneous and long-term immobilization of metal(loid)s in soil under simulated aging, *Sci. Total Environ.*, 2024, **947**, 174777.

10 Z. Shen, in *Biochar Application in Soil to Immobilize Heavy Metals*, ed. Z. Shen, Elsevier, 2024, pp. 131–162, DOI: 10.1016/B978-0-323-85459-7.00003-3.

11 L. Wang, D. O'Connor, J. Rinklebe, Y. S. Ok, D. C. W. Tsang, Z. Shen and D. Hou, Biochar Aging: Mechanisms, Physicochemical Changes, Assessment, And Implications for Field Applications, *Environ. Sci. Technol.*, 2020, **54**, 14797–14814.
12 X. Chen, S. Jiang, J. Wu, X. Yi, G. Dai and Y. Shu, Three-year field experiments revealed the immobilization effect of natural aging biochar on typical heavy metals (Pb, Cu, Cd), *Sci. Total Environ.*, 2024, **912**, 169384.
13 H. Cui, Q. Wang, X. Zhang, S. Zhang, J. Zhou, D. Zhou and J. Zhou, Aging reduces the bioavailability of copper and cadmium in soil immobilized by biochars with various concentrations of endogenous metals, *Sci. Total Environ.*, 2021, **797**, 149136.
14 F. Guo, C. Ding, Z. Zhou, G. Huang and X. Wang, Stability of immobilization remediation of several amendments on cadmium contaminated soils as affected by simulated soil acidification, *Ecotoxicol. Environ. Saf.*, 2018, **161**, 164–172.
15 K. Qiu, L. Zhao, Y. An, X. Li and Z. Zhang, Stable and efficient immobilization of lead and cadmium in contaminated soil by mercapto iron functionalized nanosilica, *Chem. Eng. J.*, 2021, **426**, 128483.
16 X. Liang, Y. Xu, X. Tan, L. Wang, Y. Sun, D. Lin, Y. Sun, X. Qin and Q. Wang, Heavy metal adsorbents mercapto and amino functionalized palygorskite: Preparation and characterization, *Colloids Surf., A*, 2013, **426**, 98–105.
17 Y. Wang, Y. Xu, X. Liang, Y. Sun, Q. Huang, X. Qin and L. Zhao, Effects of mercapto-palygorskite on Cd distribution in soil aggregates and Cd accumulation by wheat in Cd contaminated alkaline soil, *Chemosphere*, 2021, **271**, 129590.
18 H. Yang, M. Wang, X. Chen, Y. Xu, L. Zong, Q. Huang, Y. Sun, L. Wang, Y. Zhao and X. Liang, Sulfhydryl grafted palygorskite amendment with varying loading rates: Characteristic differences and dose-effect relationship for immobilizing soil Cd, *Sci. Total Environ.*, 2022, **842**, 156926.
19 Q. Huang, X. Di, Z. Liu, L. Zhao, X. Liang, S. Yuebing, X. Qin and Y. Xu, Mercapto-palygorskite efficiently immobilizes cadmium in alkaline soil and reduces its accumulation in wheat plants: A field study, *Ecotoxicol. Environ. Saf.*, 2023, **266**, 115559.
20 Y. Wu, H. Yang, M. Wang, L. Sun, Y. Xu, G. Sun, Q. Huang and X. Liang, Immobilization of soil Cd by sulfhydryl grafted palygorskite in wheat-rice rotation mode: A field-scale investigation, *Sci. Total Environ.*, 2022, **826**, 154156.
21 G. Gao, T. Sun, Y. Sun, Y. Xu and X. Liang, Adsorption of Cd(II) on mercapto-palygorskite functional materials with different proportions: Performance, mechanism and DFT study, *J. Cleaner Prod.*, 2024, **452**, 142052.
22 Z. Xia, L. Baird, N. Zimmerman and M. Yeager, Heavy metal ion removal by thiol functionalized aluminum oxide hydroxide nanowhiskers, *Appl. Surf. Sci.*, 2017, **416**, 565–573.
23 Y. Wang, Y. Xu, X. Liang, Y. Sun, Q. Huang and Y. Peng, Leaching behavior and efficiency of cadmium in alkaline soil by adding two novel immobilization materials, *Sci. Total Environ.*, 2020, **710**, 135964.
24 X. Mo, Z. Zhuang, C. Ren and W. Li, Thermal activation of palygorskite for enhanced fluoride removal under alkaline conditions, *Appl. Geochem.*, 2022, **147**, 105484.
25 X. Liu, P. Zhang, H. Liu and L. Liao, Quantitative phase analysis method of palygorskite based on XRD orientational sample analysis and Rietveld full spectrum fitting, *Appl. Clay Sci.*, 2024, **248**, 107222.
26 J. L. García Ruano, A. Parra and J. Alemán, Efficient synthesis of disulfides by air oxidation of thiols under sonication, *Green Chem.*, 2008, **10**, 706–711.
27 X. Zhou, Z. Wu, B. Chen, Z. Zhou, Y. Liang, M. He and B. Hu, Quantification of trace heavy metals in environmental water, soil and atmospheric particulates with their bioaccessibility analysis, *Talanta*, 2024, **276**, 126284.
28 J. Han, X. Liang, Y. Xu and Y. Xu, Removal of Cu^{2+} from aqueous solution by adsorption onto mercapto functionalized palygorskite, *J. Ind. Eng. Chem.*, 2015, **23**, 307–315.
29 A. Zeida and R. Radi, in *Redox Chemistry and Biology of Thiols*, ed. B. Alvarez, M. A. Comini, G. Salinas and M. Trujillo, Academic Press, 2022, pp. 99–113, DOI: **10.1016/B978-0-323-90219-9.00028-5**.
30 J. J. Kim, S. S. Lee, P. Fenter, S. C. B. Myneni, V. Nikitin and C. A. Peters, Carbonate Coprecipitation for Cd and Zn Treatment and Evaluation of Heavy Metal Stability Under Acidic Conditions, *Environ. Sci. Technol.*, 2023, **57**, 3104–3113.
31 X. Liu, M. Meng, Y. Zhang, C. Li, S. Ma, Q. Li, Q. Ren, Y. Zhang and J. Zhang, Effects of sulfuric, nitric, and mixed acid rain on the decomposition of fine root litter in Southern China, *Ecol. Process.*, 2021, **10**, 65.
32 W. Li, Y. Deng, H. Wang, Y. Hu and H. Cheng, Potential risk, leaching behavior and mechanism of heavy metals from mine tailings under acid rain, *Chemosphere*, 2024, **350**, 140995.
33 C. Zhao, J. Yao, T. Š. Knudsen, J. Liu, X. Zhu and B. Ma, Effect of goethite-loaded montmorillonite on immobilization of metal(loid)s and the micro-ecological soil response in non-ferrous metal smelting areas, *Sci. Total Environ.*, 2023, **865**, 161283.
34 G. Wang, H. Xiao, G. Liang, J. Zhu, C. He, S. Ma, Z. Shuai and S. Komarneni, Leaching characteristics and stabilization of heavy metals in tin-polymetallic tailings by sodium diethyl dithiocarbamate intercalated montmorillonite (DDTC-Mt), *J. Cleaner Prod.*, 2022, **344**, 131041.
35 Z. Huang, L. Jiang, P. Wu, Z. Dang, N. Zhu, Z. Liu and H. Luo, Leaching characteristics of heavy metals in tailings and their simultaneous immobilization with triethylenetetramine functioned montmorillonite (TETA-Mt) against simulated acid rain, *Environ. Pollut.*, 2020, **266**, 115236.
36 J. Li, B. Wu, Z. Luo, N. Lei, H. Kuang and Z. Li, Immobilization of cadmium by mercapto-functionalized palygorskite under stimulated acid rain: Stability performance and micro-ecological response, *Environ. Pollut.*, 2022, **306**, 119400.
37 X. Fang, W. Yuan, Z. Li, X. Zhang, J. Yu, J. Chen, X. Wang and X. Qiu, Effect of calcination temperatures on the

performance of rectorite for cadmium immobilization in soil: Freeze-thaw, plant growth, and microbial diversity, *Environ. Res.*, 2023, **216**, 114838.

38 X. Liang, N. Li, L. He, Y. Xu, Q. Huang, Z. Xie and F. Yang, Inhibition of Cd accumulation in winter wheat (Triticum aestivum L.) grown in alkaline soil using mercapto-modified attapulgite, *Sci. Total Environ.*, 2019, **688**, 818–826.

39 B. Wei, Y. Peng, P. Jeyakumar, L. Lin, D. Zhang, M. Yang, J. Zhu, C. S. Ki Lin, H. Wang, Z. Wang and C. Li, Soil pH restricts the ability of biochar to passivate cadmium: A meta-analysis, *Environ. Res.*, 2023, **219**, 115110.

40 Y. Yong, T. Yang, Y. Wang, Y. Xu, Q. Huang, X. Liang, Y. Sun and L. Wang, Mercapto–palygorskite decreases the Cd uptake of wheat by changing Fe and Mn fraction in Cd contaminated alkaline soil, *Geoderma*, 2024, **441**, 116751.

41 Y. Huang, B. Zhao, G. Liu, K. Liu, B. Dang, H. Lyu and J. Tang, Effective reducing the mobility and health risk of mercury in soil under thiol-modified biochar amendment, *J. Hazard. Mater.*, 2024, **462**, 132712.

42 Y. Wang, Y. Liu, W. Zhan, K. Zheng, M. Lian, C. Zhang, X. Ruan and T. Li, Long-term stabilization of Cd in agricultural soil using mercapto-functionalized nano-silica (MPTS/nano-silica): A three-year field study, *Ecotoxicol. Environ. Saf.*, 2020, **197**, 110600.

